European Review for Medical and Pharmacological Sciences 2016; 20: 3490-3499

Porous tantalum seeded with bone marrow mesenchymal stem cells attenuates steroid-associated osteonecrosis

W.-M. FU[1,2], L. YANG[2], B.-J. WANG[2], J.-K. XU[3], J.-L. WANG[3], L. QIN[3,4], D.-W. ZHAO[1,2]

[1]Southern Medical University, Guangzhou, Guangdong, China
[2]Department of Orthopedics, Dalian University Zhongshan Hospital, Dalian, Liaoning, China
[3]Department of Orthopaedics and Traumatology, The Chinese University of Hong Kong, China, Shatin, Hong Kong, China
[4]State Key Laboratory of Space Medicine Fundamentals and Application, Chinese Astronaut Research and Training Center, China

Abstract. – OBJECTIVE: Bone marrow mesenchymal stem cells (BMMSCs) have been widely applied in osteonecrosis. However, lack of biomechanical support limited application of BMMSCs. And porous tantalum (PTA) has been identified as a cell-friendly scaffold for bone regeneration. Herein, we aimed to investigate the efficacy of PTA seeded with BMMSCs in the treatment of osteonecrosis.

MATERIALS AND METHODS: After the production of PTA seeded with BMMSCs, MTT and GFP were performed to identify the proliferation and adhesion of BMMSCs respectively, which was further examined by scanning electron microscopy (SEM). And real-time PCR was also used to determine mRNA level of osteogenic markers, including Alp, OCN, OPN, Col I and Runx-2 in BMMSCs. Nineteen adult rabbits were applied for building steroid-associated osteonecrosis (SAON) models. Bone formation rate (BFR) and mineral apposition rate (MAR) were determined. And Goldner Trichrome Staining was used in these SAON models, which further confirmed the efficacy of PTA seeded with BMMSCs in SAON.

RESULTS: PTA seeded with BMMSCs showed excellent biocompatibility. Additionally, SEM assay showed that BMMSCs adhered tightly and spread fully in the pores of PTA. Next, the expression of ALP and OPN mRNA in BMMSCs were significantly ($p < 0.05$) higher in the PTA-treated group compared to those in the PTA-untreated group. Furthermore, compared to those treated by only PTA, the dynamic bone formation in rabbits treated by PTA seeded with BMMSCs was significantly increased ($p < 0.001$) at both week 3rd and week 6th.

CONCLUSIONS: The product, PTA seeded with BMMSCs, was successfully produced, and was determined as high efficacy for treatment of steroid-associated osteonecrosis. PTA seeded with BMMSCs may afford a promising option for treating osteonecrosis.

Key Words:
Porous tantalum, Bone marrow mesenchymal stem cells, Steroid-associated osteonecrosis, Implantation.

Introduction

Bone marrow mesenchymal stem cells (BMMSCs) have been widely used in tissue engineering. BMMSCs can differentiate into a variety of cell lineages, including osteoblasts, adipocytes, and chondrocytes[1,2]. Zhao et al[3] suggested that transplanted BMMSCs were applied to treat osteonecrosis, which received a promising outcome in delaying or avoiding femoral head collapse. However, lack of biomechanical support is a major drawback for BMMSCs to preventing the progression of osteonecrosis, including hip joint collapse[4,5]. Porous tantalum (PTA) serves as a cell-friendly scaffold for bone regeneration. It is reasonable for us to speculate that combining BMMSCs with PTA would achieve a better outcome in the treatment of osteonecrosis.

Metallic implants have been widely used in orthopedic treatment. And titanium (Ti) is the most widely used metal with strong mechanical property[6], which can replace the role of the bone after implantation *in vivo*. However, Ti has a high elastic modulus, which will induce stress shielding, and consequently bone loss[7]. Therefore, investiga-

Corresponding Author: Ling Qin, MD; e-mail: qinling1357@sina.com
Dewei Zhao, MD; e-mail: zhaodewei1357@sina.com

tion on potential substitutes for Ti was necessary. Tantalum (Ta) can meet the demands of weight-bearing, and its elastic modulus (quite close to the cancellous bone) is much lower than Ti. Recently, successful design of porous tantalum (PTA) allows wide application of PTA for orthopedic implant[8]. PTA is designed as three-dimensional porous structure without significant reduction in mechanical strength, and this structure is suggested to be more favorable for the growth, adhesion, and differentiation of the transplanted cells[9]. Meanwhile, the higher friction coefficient of PTA leads to better stability compared with traditional Ti[10]. Ever since 1997, PTA has received approval from the Food and Drug Administration (FDA) in the USA as an optional treatment for osteonecrosis at an early stage. Promising effect was found in the early small-scale clinical trial[11,12], but failed in the subsequent large-scale clinical trial[13]. Thus, it requires further investigation on the application of PTA for the treatment of osteonecrosis, using animal models or continuing well-controlled clinical trial.

In the current study, we aimed to confirm the biocompatibility of PTA, and investigate the efficacy of PTA seeded with BMMSCs for the treatment of osteonecrosis. We tested the proliferation and adhesion of BMMSCs on the surface of PTA *in vitro*. Real-time PCR was also applied to measure the differentiation of BMMSCs. After confirming that PTA is a suitable scaffold for maintaining the survival and differentiation of BMMSCs, we further evaluated the potential of PTA seeded with BMMSCs in attenuating the progression of steroid-associated osteonecrosis (SAON) in the femoral head of a rabbit. Our results indicated that PTA seeded with BMMSCs afforded a promising option for treating osteonecrosis.

Materials and Methods

Fabrication of PTA

The PTA was produced according to the protocol (China Patent No ZL2013I0447227.6; ZL2013I0444808.4). In brief, commercially pure tantalum was fabricated onto a vitreous carbon scaffold via carbon vapor deposition/infiltration, to achieve the structure of repeating dodecahedrons. The fabricated metal possessed the following properties: porosity (70%-80%), elastic modulus (~3 MPa). Parameters were further confirmed by scanning electronic microscopy (SEM). Then, these large PTA blocks were cut into small cylinders with 5 mm in diameter, and 8 mm in height (this size is suitable for further *in vivo* experiments). These cylinders were sterilized by autoclaving prior to cell seeding.

Isolation and Culture of BMMSCs

BMMSCs were isolated from 3-month-old New Zealand rabbit (with ~2.0 kg body weight) as previously described[14]. In brief, under intramuscular anesthesia [ketamine (10 mg/kg) and xylazine (3 mg/kg)] in rabbits, bone marrow was isolated from the femur, and the isolated BMMSCs were cultured in α-MEM (Gibco, Waltham, MA, USA) with 10% fetal bovine serum (FBS, Gibco, USA) in an incubator for 37 °C, 5% CO_2, and 100% humidity, as described previously[14]. The cells used in the subsequent tests were at Passage 3rd-5th, which have been confirmed as the most suitable objects.

Proliferation Assay of BMMSCs

PTA and Ti were autoclaved for 1 h. According to the test guideline[15], the standard dilution ratio for the surface area of the sample to cell culture medium was 3 cm^2/ml. And the extracted solutions were made by soaking the specified material in sterile conditions of 37 °C, 5% CO_2 and 100% humidity, for 72 hours[15]. The initial density of BMMSCs was 4000 cells/well in 96-well plates. After incubating the cells for another 24 hours in complete α-MEM, the medium was changed into the diluted solutions or basal complete culture medium. Then MTT tests were performed at 24th hour and 48th hour post-treatment, respectively.

Cell Adhesion in PTA

Three PTA cylinders were placed in the 12-well plate, respectively. The cells (2.0×10^4 cells) were seeded onto the materials. The medium was changed every two days. At day 2nd, day 5th and day 7th, GFP (Life Technology, Waltham, MA, USA) was used to stain the cells adhered onto the materials, respectively. Cells adhesion was observed under the fluorescence microscopy (Zeiss, Jena, Germany).

Scanning Electron Microscopy (SEM)

SEM was used to examine the adhesion and differentiation of BMMSCs cultured into the PTA pores or on surfaces. PTA scaffolds were placed into 6-well plates, with one cylinder per well. We washed the materials with phosphate-buffered saline (PBS) for twice, and then seeded

cell suspension (containing 2.0 x 10^4 cells). The cultures were incubated at 37 °C with 5% CO_2. The culture medium was changed every two days. At day 2nd, day 5th and day 7th, these PTAs were taken out respectively. The loosely adherent or unbound cells from the experimental wells were removed by aspiration, the PTAs were washed twice with PBS, and the remaining bound cells were fixed in 4% paraformaldehyde in PBS for 15 min. The fixative was then aspirated. After washed with PBS, the PTAs were dehydrated in a graded series of ethanol solutions. After critical point drying (HCP-2, Hitachi, Tokyo, Japan), the samples were sputtered with Au/Pd using an SEM coating system (Quorum Q150T-S, Quorum Technologies, West Sussex, UK), and the probes were examined by field emission-SEM (FE-SEM; Hitachi S-4700, Hitachi) at 15.0 kV.

RNA Extraction and Real-Time RT-PCR

This included four experimental groups, three replicates for each group. The first group was BMMSCs group, the second group was PTA with BMMSCs group, the third group was bone induction group, and the fourth group was bone induction with PTA group. Then six PTAs were placed in six wells respectively, which was a metal group as control. The second generation of BMMSCs were digested by trypsin and then putted into a sterile tube; the cell number was adjusted to 2.0×10^4 for every dish, and then putted them into the incubator. The medium was changed every two days until BMMSCs overgrew on the well bottom. The bone induction group and bone induction with PTA group were subjected to induction medium (dexamethasone, 10 μl/100 ml; ascorbate-2-phosphate, 100 μl/100 ml; Glycerol-2-phosphate-disodium salt hydrate, 1000 μl/100 ml). The other groups were subjected to normal cell culture medium. The medium was changed every two days during three weeks of culture. After washing with PBS for twice, cell lysis solution was added into 12-well plates. The cells were then repeated pipetting down from the board and PTAs respectively. Total RNA was extracted from the separated aqueous phase with RNA Tissue Kit SII on the QuickGene extraction robot (Fujifilm Life Science, Tokyo, Japan) according to manufacturer's instructions. All RNA samples were analyzed for RNA quantity with Nano Drop ND-1000 spectrophotometer (Thermo Scientific Nano Drop Technologies, Wilmington, DE, USA). All RT was performed using Script cDNA Synthesis kit (Bio-Rad Laboratories, Hercules, CA, USA) to generate cDNA for relative quantification on mRNA. After reverse transcription, cDNA samples were stored in -20 °C. Real-time quantitative reverse transcription (RT-PCR) with custom-designed primers (Tech Dragon Co., Ltd, Hong Kong, China) was performed in 20 μl reaction in triplicate for each sample (Table I).

In vivo Test the Efficacy of PTA Seeded with BMMSCs in the Treatment of SAON Model

Totally nineteen healthy adult rabbits (six-month-old, male) were used in our study. All animal procedures were approved by the Institutional Animal Care and Use Committee at the Chinese University of Hong Kong. All the experimental procedures were strictly performed according to the approved guidelines. SAON model was established using our published protocol[16]. In brief, all the animals received one intravenous injection of 10 μg/kg lipopolysaccharide (LPS, Sigma-Aldrich, Inc., St. Louis, MO, USA). Twenty-four hours later, three injections of 20 mg/kg methylprednisolone (MPS, Pharmacia & Upjohn, Peapack, NJ, USA) were given intramuscularly at a time interval of 24 h. Two weeks later, three animals were sacrificed for harvesting bilateral femoral heads to confirm that osteonecrosis model has been successfully established. The rest sixteen animals were injected with MPS, and two weeks later these animals were randomly divided into two groups (n = 8/group), including PTA seeded with BMMSCs group, and PTA without BMMSCs group. The rabbits were anesthetized with xylazine (2 mg/kg body weight) and ketamine (50 mg/kg body weight). At day 3rd and day 10th before sacrificed,

Table I. Primer sequences used for real-time RT-PCR.

Gene	Primer sequences
ALP	5'–TGGACCTCGTGGACATCTG'–3' (F)
	5'–CAGGAGTTCAGTGCGGTTC–3' (R)
OPN	5'–ACAAGAGACCCTCCCGAGTA–3' (F)
	5'–GTCGGATTCATTGGAGTCCT–3' (R)
OCN	5'–CTCACTCTGCTGGCCCTGAC–3' (F)
	5'–CCTTACTGCCCTCCTGCTTG–3' (R)
RUNX-2	5'–TACTGTCATGGCGGGTAATG–3' (F)
	5'–AGGTGAAACTCTTGCCTCGT–3' (R)
GAPDH	5'–TCTGGCAAAGTGGATGTTGT–3' (F)
	5'–GTGGGTGGAATCATACTGGA–3' (R)

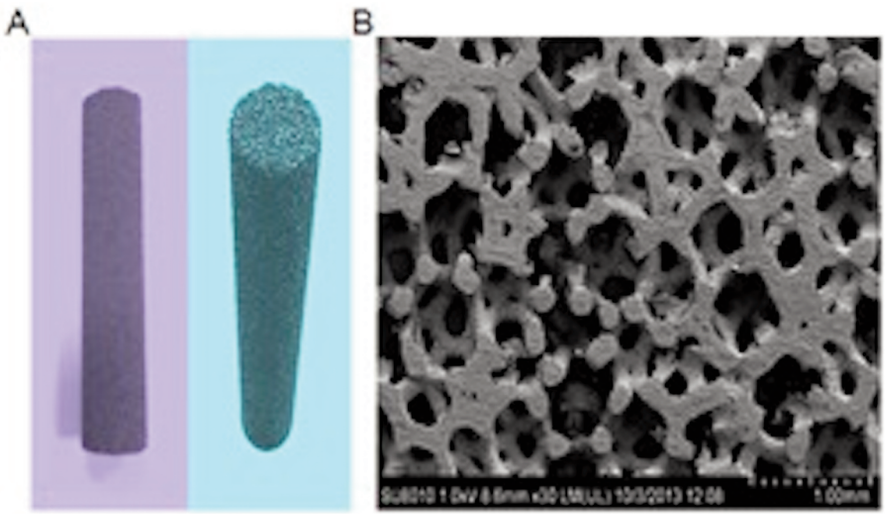

Figure 1. Macroscopic performance of the fabricated cylindrical PTA in ***(A)*** its original form, and ***(B)*** representative SEM image showing the porosity of PTA.

animals were injected with green (calcein green) and red (xylenol red) fluorescent calcium-binding dye, which could label new bone deposition at bone-formation site, respectively, according to our published protocol[17]. Four animals from each group were sacrificed at week 3rd and week 6th, respectively. The femoral heads were harvested and embedded with methylmethacrylate (MMA) for hard tissue sectioning.

Calculation of Bone Formation Rate (BFR) and Mineral Apposition Rate (MAR)

Polished 100 μm thick MMA sections were observed using a microscope (model DMLB; Leica, Oskar, Germany), 3 CCD color video DXC-390 camera (Sony) and the OsteoMeasure Analysis System (OsteoMetrics, Atlanta, GA, USA). Kinetic index, including BFR and MAR were measured for bone histomorphometry[18].

Goldner Trichrome Staining

For dynamic histology, undecalcified samples embedded in MMA were cut into 200 μm thick sections. Then the sections were polished into 50 μm thick. The osteoid area was measured by Goldner Trichrome staining and analyzed using OsteoMeasure image analysis software (OsteoMetrics, Atlanta, GA, USA).

Statistical Analysis

All the quantitative data were expressed as mean ± SD ($n \geq 3$ for each experiment). Graphpad Prism software (version 6.0) was used for statistical analysis. Two groups were compared by using two independent sample *t*-test. For comparison in multiple groups, One-way ANOVA was used. $p < 0.05$ was considered as statistically significant.

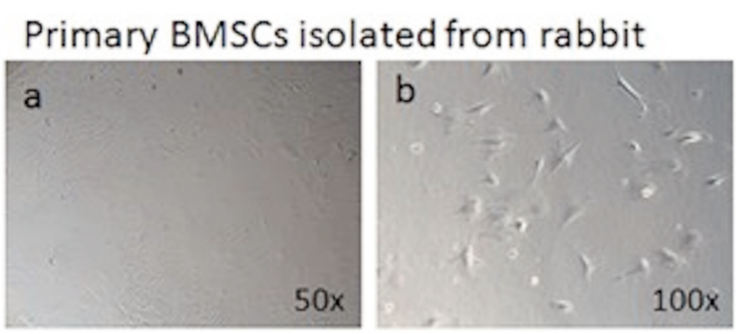

Figure 2. Morphology of the isolated BMMSCs under magnification of x 50 ***(A)*** and x100 ***(B)***.

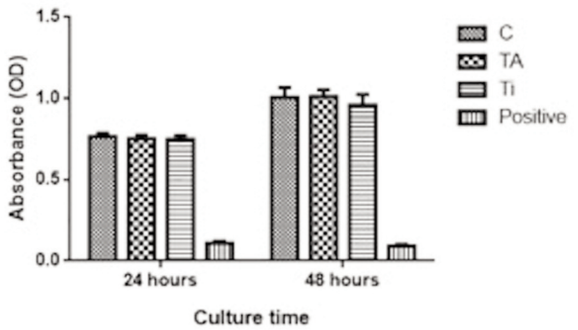

Figure 3. Quantitative analysis of cell proliferation using MTT test (N = 6).

Results

Biomaterial Properties of Fabricated PTA was Confirmed for Commercial Application

Figure 1A showed the gross view of our fabricated PTA. The results from SEM indicated that the PTA was of high volumetric porosity (around 80%) (Figure 1B), which was similar to commercial porous tantalum[19].

Good Biocompatibility of PTA for BMMSCs

Rabbit BMMSCs were successfully isolated and cultured (Figure 2A, 2B). Cell proliferation assay showed that the proliferation of BMMSCs in the extracted solution of PTA grew the same as that of those cultured in complete culture medium or extraction from Ti (Figure 3), which indicated that our fabricated PTA was of good biocompatibility.

Morphology of BMMSCs on the Surface of PTA

GFP cells were used to investigate if the morphology of BMMSCs was altered when cultured on PTA. Bright field image showed the normal morphology of BMMSCs in a plastic culture dish (Figure 4A). GFP-positive cells were showed in Figure 4B. And BMMSCs seeded onto the surface of PTA were recorded using a fluorescent microscope (Figure 4C). At day 2nd, only some scattered green dots could be detected (Figure 4C-c1, c2). At day 5th, more cells could be observed with increased area of cells adhered onto the surface of PTA (Figure 4C-c3, c4), and cells at day 7th grew more (Figure 4C-c5, c6). As the enhancement in adhesion and spreading of MSCs can lead to promotion in osteogenesis[20], our results indicated that PTA was favorable for

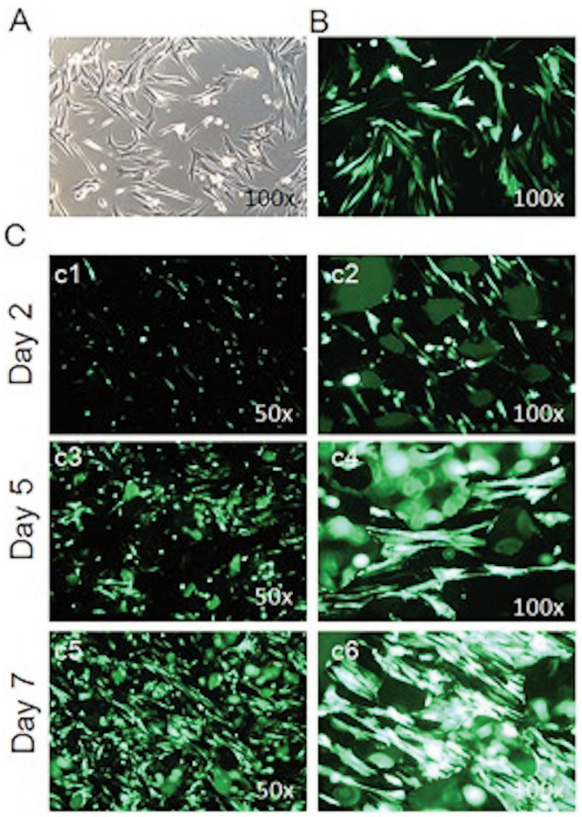

Figure 4. Comparison of cell morphology seeding with or without PTA. ***(A-B)*** GFP-positive cells were observed under a magnification of x 100. ***(C)*** Representative fluorescent images showed the change of cell morphology over time.

transplanted BMMSCs to promote the osteogenesis. A consistent result was observed using SEM (Figure 5). Co-cultured of PTA with BMMSCs for 2 days, we observed few BMMSCs adhesion to either the surface or the dispersing pores of PTA (Figure 5A). Co-cultured of PTA with BMMSCs for 5 days, the number of cells increased significantly, which indicated that these BMMSCs were undergoing proliferation (Figure 5B). Co-cultured of PTA with BMMSCs for 7 days, we observed a lot of BMMSCs adhered to the inner surface as well as the porous of PTA (Figure 5C).

The Osteogenesis of BMMSCs is Enhanced when Seeded with PTA

The expressions of *OCN* and *OPN* mRNA in BMMSCs ($p < 0.05$; Figure 6A, 6B) were detected by real-time PCR. And the expression was significantly higher in the pores of PTA than those cultured in osteogenic induction medium,

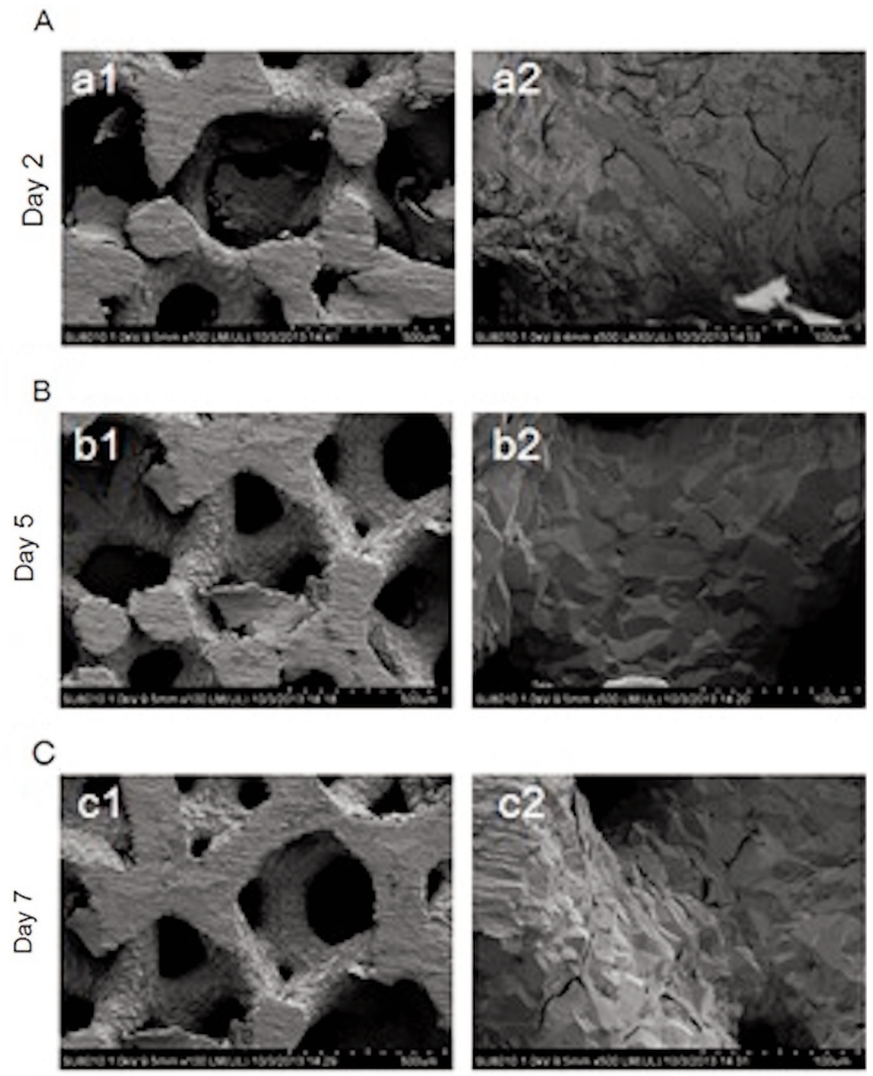

Figure 5. Representative SEM images of PTA seeded with BMMSC at day 2nd ***(A)***, day 5th ***(B)***, and day 7th *(C)*.

which indicated that BMMSCs in pores of PTA showed comparable osteogenic differentiation ability. BMMSCs surrounding PTA also have a good potential osteogenic differentiation, with an increase in *ALP* and *Runx-2* gene expression levels ($p < 0.05$; Figure 6C, 6D). In addition, we also examined the expression of type I collagen mRNA, but there is no statistical difference between these groups (Figure 6E). Perhaps, the reason was that the collected specimens were just for the early stage of osteogenesis, and type I collagen is a marker for the late stage of osteogenic differentiation. In conclusion, the BMMSCs with PTA performed more potential for the osteogenic differentiation.

Bone Formation is Increased in SAON Model Treated with PTA Seeded with BMMSCs

Our study further investigated the efficacy of PTA seeded with BMMSCs on SAON model. To investigate the dynamic bone formation, we used calcein green and xylenol orange to sequentially label the regenerated osteoid. We found more extensively calcein and xylenol labeling and a larger width between two labeling bands in PTA seeded with BMMSCs group compared to those in PTA without BMMSCs group (Figure 7A). The quantification of the distance between the xylenol and calcein labeling was also reflected in the bone-formation-

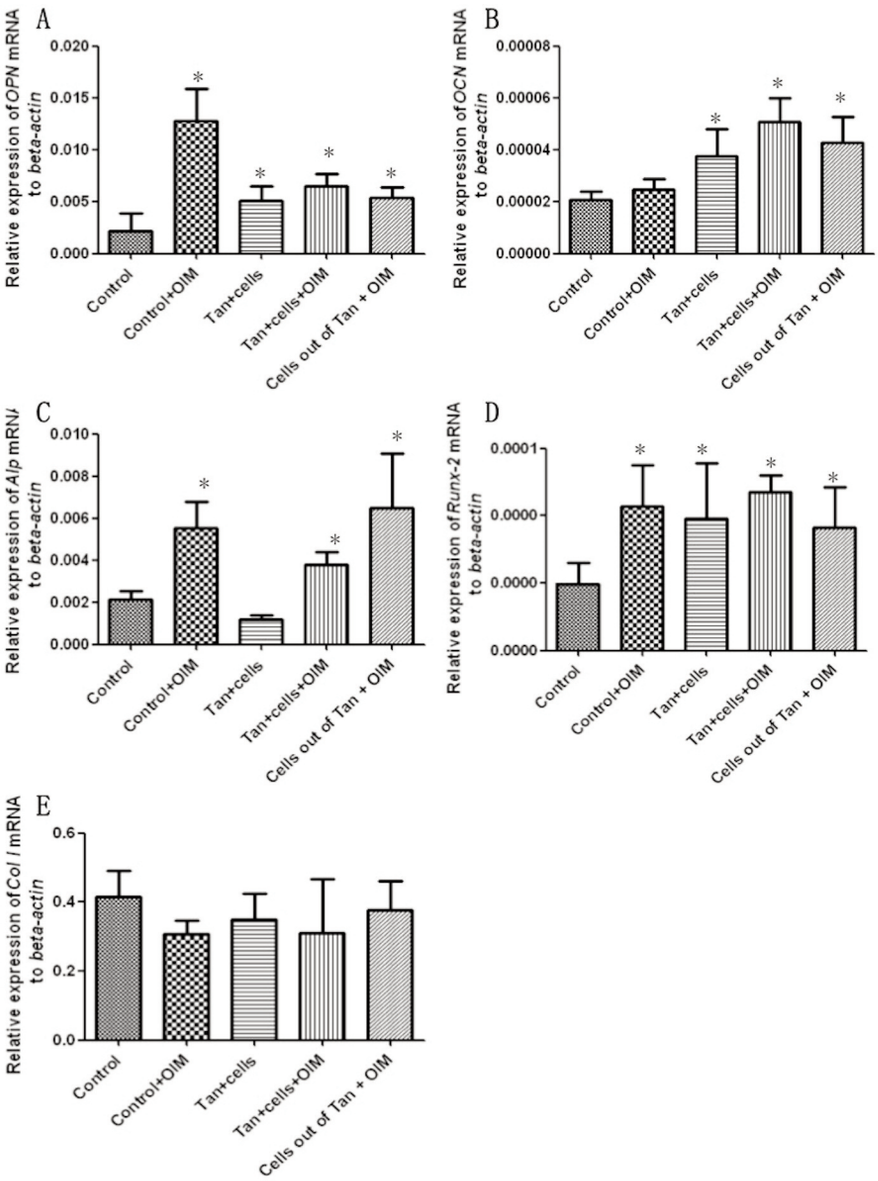

Figure 6. The mRNA expression levels of osteogenic markers, including ***(A)*** Alp, ***(B)*** OCN, ***(C)*** OPN, ***(D)*** Col I and (E) Runx-2 in BMMSCs. *$p < 0.05$ presented as statically significance.

related parameters, including MAR (Figure 7B) and BFR (Figure 7C). In addition, Goldner Trichrome Staining also showed that there was significantly more new bone formation in PTA with BMMSCs group compared to that in PTA without BMMSCs group (Figure 8A). Quantitative measurement of the total tissue area showed that newly regenerated bone tissue was increased at either week 3rd or week 6th (Figure 8B), while there was increased of osteoid at only early time point, including week 3rd (Figure 8C). All these results suggested that PTA seeded with BMMSCs could serve as a better option for the treatment of SAON.

Discussion

The mechanical properties and porous structure of the Tantalum have been investigated for decades[21]. Tantalum has the advantages of great strength, suitable elastic modulus ranging be-

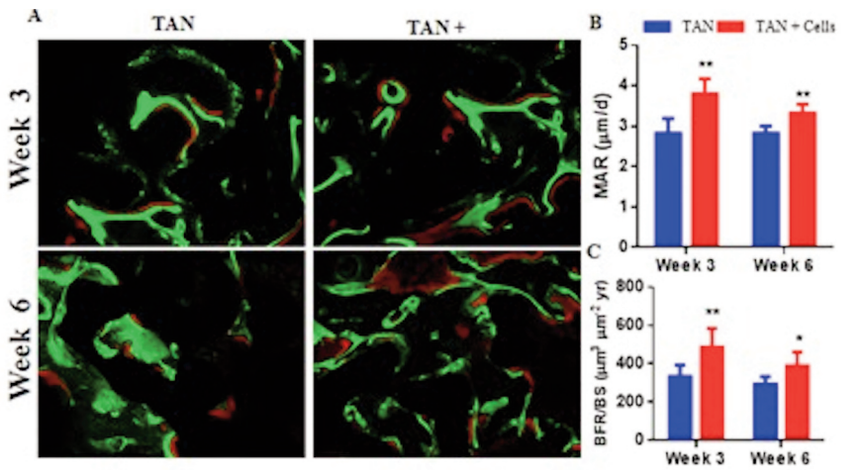

Figure 7. Dynamic bone formation in animal models receiving different treatments. ***(A)*** Representative fluorescent images from non-calcified bone sections showed significantly increased labeling area and width, with an increase in MAR ***(B)*** as well as BFR (C). N = 5/group/time point. $^{*}p < 0.05$, $^{**}p < 0.01$ presented as statically significance.

tween cortical bone and cancellous bone, which makes the stress shielding significantly lower compared to Ti. PTA with 75%-80% porosity has been determined to be favorable for cell growth and proliferation[22]. T [3]hough PTA has been used in the treatment of osteonecrosis in clinical practice for more than ten years, the outcome is far from expected[23]. Despite the PTA can provide effective mechanical support and good cell growth environment, the unsatisfactory outcome is likely resulted from that insufficient cells grew in the pores of PTA.

BMMSCs are considered as one of the most promising seed cells for tissue engineering[24-27], including application in the treatment of osteonecrosis. At present, a large number of clinical

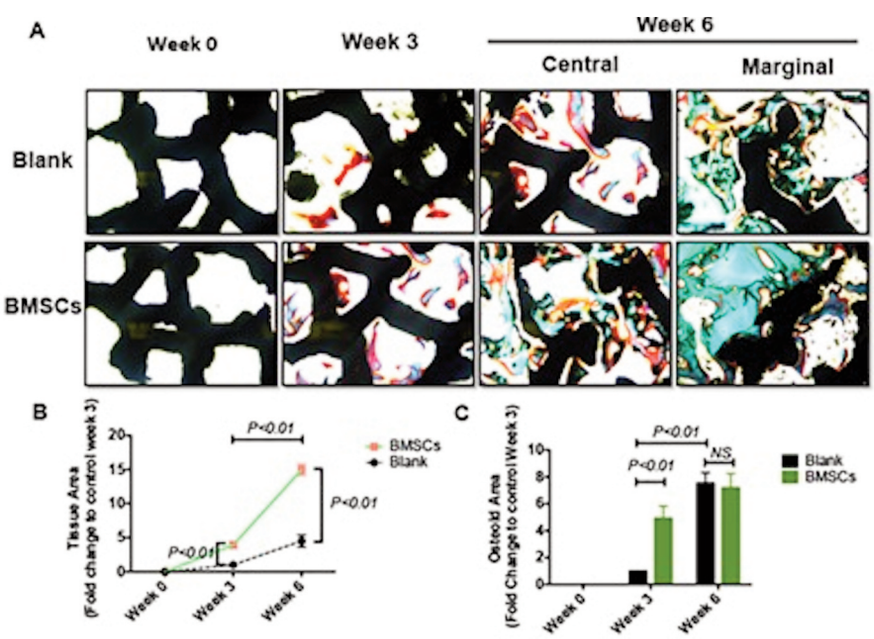

Figure 8. Goldner Trichrome staining of the bone-like tissue within the pores as well as the surrounding of PTA. ***(A)*** Newly formed bone was stained with red, while mineralized bone matrix was stained with green. Quantitative measurement of total regenerated tissue (*in red and green*) and osteoid positive area (*in red only*) were performed. And the results were summarized as ***B*** and ***C*** in Figure 8.

reports confirmed that BMMSCs were of great potential for the treatment of early osteonecrosis. Hernigou et al[25] used core decompression combined with autologous BMMSCs transplantation to treat osteonecrosis in the femoral head, and finally determined that only 3% Phase I and 8% Phase II osteonecrosis needed a hip replacement after 5-10 years of follow-up. Juan et al[26] have successfully used PTA combined with BMMSCs to increase the spinal fusion rate. Moreover, in the treatment of osteonecrosis, there are many reports for a single application with PTA or BMMSCs[27], but until now few report is available about the combination of PTA and BMMSCs for osteonecrosis. To our knowledge, it is the first time that we used PTA seeded with BMMSCs to treat SAON.

Conclusions

Our study demonstrated that our fabricated PTA is of good biocompatibility in the promotion of BMMSCs adhesion and differentiation on the surface or within the pores. PTA seeded with BMMSCs showed a superior therapeutic effect in attenuating the progress of SAON, presenting with the significantly more new bone formation.

Acknowledgements

This work was supported by National Natural Science Foundation (30970699) and National Science and Technology Support Program (2012BAI17B02).

Conflict of Interest

The Authors declare that they have no conflict of interests.

References

1) Izal I, Aranda P, Sanz-Ramos P, Ripalda P, Mora G, Granero-Moltó F, Deplaine H, Gómez-Ribelles JL, Ferrer GG, Acosta V. Culture of human bone marrow-derived mesenchymal stem cells on of poly (L-lactic acid) scaffolds: potential application for the tissue engineering of cartilage. Knee Surg Sports Traumatol Arthrosc 2013; 21: 1737-1750.
2) Liang Y, Cao R. Employment assistance policies of Chinese government play positive roles! The impact of post-earthquake employment assistance policies on the health-related quality of life of Chinese earthquake populations. Social Indicators Res 2015; 120: 835-857.
3) Li Y, Wang K, Zou QY, Magness RR, Zheng J. 2,3,7,8-Tetrachlorodibenzo-p-dioxin differentially suppresses angiogenic responses in human placental vein and artery endothelial cells. Toxicology 2015; 336: 70-78.
4) Zheng LZ, Liu Z, Lei M, Peng J, He YX, Xie XH, Man CW, Huang L, Wang XL, Fong DTP. Steroid-associated hip joint collapse in bipedal emus. PLoS One 2013; 8: e76797.
5) Liang Y, Lu P. Health-related quality of life and the adaptation of residents to harsh post-earthquake conditions in China. Disaster Med Public Health Prep 2014; 8: 390-396.
6) Li Y, Wang K, Zou QY, Zhou C, Magness RR, Zheng J. A possible role of Aryl hydrocarbon receptor in spontaneous preterm birth. Med Hypotheses 2015; 84: 494-497.
7) Noyama Y, Miura T, Ishimoto T, Itaya T, Niinomi M, Nakano T. Bone loss and reduced bone quality of the human femur after total hip arthroplasty under stress-shielding effects by titanium-based implant. Materials Transactions 2012; 53: 565-570.
8) Li Y, Zhao YJ, Zou QY, Zhang K, Wu MY, Wang K, Zheng J. Vascular growth and endothelial junction protein expression in human placentas from the normal term and preeclamptic pregnancies. J Histochem Cytochem 2014; 62: 347-354.
9) Lapia MM, Chen Z, Liu F, Ahmed S and Fan W. Treatment of early osteonecrosis of femoral head: a review of femoral head sparing procedures. Sci Lett 2016; 4: 9-16.
10) Lee JW, Wen HB, Battula S, Akella R, Collins M, Romanos GE. Outcome after placement of tantalum porous engineered dental implants in fresh extraction sockets: a canine study. Int J Oral Maxillofac Implants 2015; 30: 134-142.
11) Liu Y, Su X, Zhou S, Wang L, Wang C, Liu S. A modified porous tantalum implant technique for osteonecrosis of the femoral head: survivorship analysis and prognostic factors for radiographic progression and conversion to total hip arthroplasty. Int J Clin Exp Med 2015; 8: 1918.
12) Liang Y, Wu W. Exploratory analysis of health-related quality of life among the empty-nest elderly in rural China: An empirical study in three economically developed cities in eastern China. Health Qual Life Outcomes 2014; 12: 59.
13) Tanzer M, Bobyn J, Krygier J, Karabasz D. Histopathologic retrieval analysis of clinically failed porous tantalum osteonecrosis implants. J Bone Joint Surg 2008; 90: 1282-1289.
14) Tan Q, Lui PPY, Rui YF, Wong YM. Comparison of potentials of stem cells isolated from tendon and bone marrow for musculoskeletal tissue engineering. Tissue Eng Part A 2011; 18: 840-851.
15) Iso E. Biological evaluation of medical devices-Part 5: tests for cytotoxicity: in vitro methods. German version EN ISO 1999; 10993-10995.
16) Qin L, Zhang G, Sheng H, Yeung K, Yeung H, Chan C, Cheung W, Griffith J, Chiu K, Leung K. Multiple bioimaging modalities in evaluation of an experi-

mental osteonecrosis induced by a combination of lipopolysaccharide and methylprednisolone. Bone 2006; 39: 863-871.

17) Zhang G, Guo B, Wu H, Tang T, Zhang BT, Zheng L, He Y, Yang Z, Pan X, Chow H. A delivery system targeting bone formation surfaces to facilitate RNAi-based anabolic therapy. Nat Med 2012; 18: 307-314.

18) Dempster DW, Compston JE, Drezner MK, Glorieux FH, Kanis JA, Malluche H, Meunier PJ, Ott SM, Recker RR, Parfitt AM. Standardized nomenclature, symbols, and units for bone histomorphometry: a 2012 update of the report of the ASBMR Histomorphometry Nomenclature Committee. J Bone Miner Res 2013; 28: 2-17.

19) Balla VK, Bodhak S, Bose S, Bandyopadhyay A. Porous tantalum structures for bone implants: fabrication, mechanical and in vitro biological properties. Acta Biomater 2010; 6: 3349-3359.

20) Dalby MJ, Gadegaard N, Oreffo RO. Harnessing nanotopography and integrin-matrix interactions to influence stem cell fate. Nat Mater 2014; 13: 558-569.

21) Bencharit S, Byrd WC, Altarawneh S, Hosseini B, Leong A, Reside G, Morelli T, Offenbacher S. Development and applications of porous tantalum trabecular metal-enhanced titanium dental implants. Clin Implant Dent Relat Res 2014; 16: 817-826.

22) Wang Q, Zhang H, Li Q, Ye L, Gan H, Liu Y, Wang H, Wang Z. Biocompatibility and osteogenic properties of porous tantalum. Exp Ther Med 2015; 9: 780-786.

23) Zhang X, Wang J, Xiao J, Shi Z. Early failures of porous tantalum osteonecrosis implants: a case series with retrieval analysis. Int Orthop 2016; 1: 1-8.

24) Elkhenany H, Amelse L, Lafont A, Bourdo S, Caldwell M, Neilsen N, Dervishi E, Derek O, Biris AS, Anderson D. Graphene supports in vitro proliferation and osteogenic differentiation of goat adult mesenchymal stem cells: potential for bone tissue engineering. J Appl Toxicol 2015; 35: 367-374.

25) Roseti L, Serra M, Canella F, Munno C, Tosi A, Zuntini M, Pandolfi M, Sangiorgi L, Biso P, Pittalis MC, Bini C, Pelotti S, Gasbarrini A, Boriani L, Bassi A, Grigolo B. In vitro gene and chromosome characterization of expanded bone marrow mesenchymal stem cells for musculo-skeletal applications. Eur Rev Med Pharmacol Sci 2014; 18: 3702-3711.

26) Li Y, Xue F, Xu SZ, Wang XW, Tong X, Lin XJ. Lycopene protects bone marrow mesenchymal stem cells against ischemia-induced apoptosis in vitro. Eur Rev Med Pharmacol Sci 2014; 18: 1625-1631.

27) Zhang T, Shao H, Xu Ko, Kuang Lt, Chen Rf, Xiu Hh. Midazolam suppresses osteogenic differentiation of human bone marrow-derived mesenchymal stem cells. Eur Rev Med Pharmacol Sci 2014; 18: 1411-1418.

25) Hernigou P, Poignard A, Zilber S, Rouard H. Cell therapy of hip osteonecrosis with autologous bone marrow grafting. Ind J Orthop 2009; 43: 40.

26) Blanco JF, Sánchez-Guijo FM, Carrancio S, Muntion S, García-Briñon J, del Canizo MC. Titanium and tantalum as mesenchymal stem cell scaffolds for spinal fusion: an in vitro comparative study. Eur Spine J 2011; 20: 353-360.

27) Chotivichit A, Korwutthikulrangsri E, Auewarakul C, Sarirasririd S. Core decompression and concentrated autologous bone marrow injection for treatment of osteonecrosis of the femoral head. J Med Assoc Thai 2012; 95: S14-20.